

Computational Investigation of Effects of Ligand Architecture on Homolytic Bond Cleavage and Electronic Structure of Molecular Bismuth Compounds

I. Introduction

Transition metals are widely used in a variety of catalytic reactions due to their excellent ability to undergo redox cycles and facilitate complex bond transformations. The exceptional ability of transition metal catalysts originates from single-electron transfer ratios, triggering radical reactions (Demarteau et al., 2016). Such catalysts are essential in both industrial and academic synthetic chemistry because of high efficiency and broad substrate scope. Nevertheless, many transition-metal catalysts are expensive, toxic, and not environmentally-friendly; for example, many transition metals such as palladium have shown to have detrimental effects on overall human health such as hepatitis, myocarditis, and rheumatoid arthritis (Jomova et al., 2024). Such factors limit sustainable use and poses challenges for green chemistry applications

Thus, the recent efforts have focused on developing main-group metal complexes as sustainable alternatives to transition-metal catalysts. While main-group elements have traditionally minor roles in redox catalysis, carefully designed ligand frameworks impart redox activity and stability to such metals (Lichtenberg, 2020). Specifically, sterically demanding and chelating ligands protect the metal center, controlling geometric constraints and electronic environment, while redox-active ligands enable reversible electron transfer without the requirement for inherently redox-active metals. Furthermore, delocalization of spin density in π -conjugated electron systems enables selective bond formation and facilitates multi-electron transformations, historically reserved for transition metals (Lichtenberg, 2020). Recent advances in ligand design have enabled main-group elements such as aluminum, boron, and silicon to participate in oxidative addition and reductive elimination pathways, mimicking transition-metal-like reactivity (Crimmin et al., 2018). These developments highlight the growing potential of main-group metal catalysts as a sustainable and cost-effective alternative to traditional transition-metal systems.

Bismuth, one of the main-group elements, offers an especially promising alternative to transition metal catalysts. The safety of bismuth is evidenced by its widespread use in pharmaceutical ingredients such as bismuth subsalicylate and colloidal bismuth subcitrate, which are utilized for their antimicrobial properties (Gonçalves et al., 2024). Additionally, bismuth is cheaper than many transition metals despite its abundance analogous to silver and mercury. Considerable quantities of bismuth are recovered as by-products of copper and tin refining, further enhancing its economic accessibility and viability as a potentially applicable catalyst in the industry (Suzuki et al., 2001). These studies highlight versatility, low toxicity, and recyclability of bismuth, suggesting Bismuth as a viable main-group metal alternative for transition metals in sustainable catalysis. Developing organobismuth catalysts could significantly

improve sustainable and efficient catalyst use, reducing reliance on expensive and toxic transition metals while expanding the toolbox for synthetic chemists. Understanding the structure, stability, and reactivity of these complexes is therefore critical for advancing greener chemistry.

Many current studies have focused on mechanistic investigations of bismuth-mediated redox catalysis, examining how electronic structure and oxidation states influence reaction pathways. Specifically, bismuth is shown to be effective in mediating redox catalysis due to its access to multiple oxidation states—Bi(III)/Bi(I), Bi(III)/Bi(II), and even Bi(V)/Bi(III)—enabling diverse radical and redox transformations (Cornella & Moon, 2022). For example, Bi(III)/Bi(I) redox cycles enable radical polymerization, photocatalysis, hydrodefluorination, and other transformations (Cornella & Moon, 2022). Among many mechanistic studies, the generation of reactive Bi-centered radicals through homolytic Bi-ligand bond cleavage is worth noting due to its ability to initiate C(sp³)-C(sp) cyclic actions and photochemically or thermally induced hydro coupling reactions (Ramler et al., 2022; Martínez, 2025).

According to mechanistic studies, these transformations often proceed via single-electron transfer processes, where radical intermediates mediate bond formations and regenerate the catalytically active bismuth species (Yang et al., 2023). Nevertheless, such pathways are frequently complicated by side reactions, including intramolecular H₂ evolution in organobismuth dihydrides or dimerization of Bi(II) radicals; to mitigate such issues, bulky ligand frameworks have been employed to provide steric protections, stabilizing the Bi-H bond and preventing radical dimerization (Kurumada et al., 2025; Lichtenberg, 2020). Despite such efforts, the dihydride intermediate remains thermally unstable above 0 °C, highlighting the intrinsic challenges in catalyst design (Kurumada et al., 2025). Consequently, many contemporary researches emphasize the design of optimal ligand architectures to stabilize the molecular complex and suppress undesired side reactions.

Several ligand frameworks have been developed to promote the formation and stabilization of Bi-centered radicals through homolytic Bi-X bond cleavage. One example is bismuth (III) diaryl alkoxide with bis(benzyl)thioether ligand, [Bi((C₆H₄CH₂)₂S)OPh]. The (C₆H₄CH₂)₂S moiety is a bulky, electron-donating group providing steric protection around the Bi center and modulates the electronic environment of the Bi-O bond (Ramler et al., 2022). Such structural motifs facilitate homolytic Bi-O cleavage under photochemical conditions, as confirmed by TEMPO radical trapping experiments, and enable reversible heterolytic cleavage under thermal conditions in the presence of phenol (Ramler et al., 2022). The bis(benzyl)thioether ligand thus simultaneously stabilizes the Bi(II) radical kinetically and tunes the redox profile of the Bi(II)/Bi(III) system via σ-donation.

Another distinct strategy involves synthesis of Bi-Mn heterobimetallic complexes designed for thermal homolytic cleavage of weak Bi-Mn bonds (Martinez et al., 2025). The resulting Bi(II) and Mn(I) species act cooperatively to mediate intramolecular C(sp³)-C(sp) cyclization of alkyl iodides tethered to alkynes. Here, the Mn center functions as a redox partner,

while the heterometallic architecture provides an intrinsic single-electron transfer pathway, enabling controlled radical invitation.

Consequently, these ligand architectures demonstrate how steric protection, electronic tuning, and metal-metal cooperation stabilize highly reactive Bi-centered radicals. In particular, electron-donating substituents enhance radical delocalization, and π -conjugated frameworks facilitate spin density distribution across the ligand, minimizing localized radical character at the bismuth center. The general principles for stabilization of such complexes rely heavily on the electronic properties of the ligands: electron-donating substituents enhance radical delocalizations, while π -conjugated frameworks facilitate spin density distribution across the ligand, minimizing localized radical character at the bismuth center. Such principles guide further studies on the radical design of ligands, enabling controlled Bi-X bond homolysis and robust catalytic radical reactivity.

Building on these design principles and previously reported ligand architectures, the incorporation of additional electron-donating substituents on phenyl rings is expected to further enhance the stability and reactivity of Bi-centered radicals. Accordingly, the goal of this research is to identify optimal ligand designs by systematically introducing substituent groups which maximize radical delocalization and steric protection. The computational studies will be employed to evaluate such modifications, and the methodology for such an approach is detailed in the following methodology section.

The primary research question is: How do different substituents ($-F$, $-NH_2$, $-OCH_3$, $-CH_3$, $-SCH_3$, $-NO_2$), their positions on the aryl rings (ortho, para, or meta depending on bridging), and the presence of bridging groups ($-CH_2$, $-S$, $-SO_2$) influence the electronic structure, quasi-atomic orbital (QUAO) profiles, and homolytic bond dissociation energies in organobismuth complexes?

II. Methodology

II.1 Candidates for Computational Screening

Based on previous DFT studies of organobismuth complexes with various ligands, the optimal molecular structures were identified by comparing the homolytic bond dissociation energies (BDE) of Mn-Bi bonds (Martinez, 2025). The BDE was calculated from single-point energies of optimized singlet and doublet states before and after the homolytic cleavage. The most favorable ligand candidates are shown in **Figure 1**. Among these, **Compound 3**, featuring methyl bridge between phenyl groups, exhibits the lowest BDE of 26.4 kcal mol⁻¹ (Martinez, 2025). Other geometries such as **Compound 2** and **4** show slightly higher BDEs of 26.8 kcal mol⁻¹ and 26.7 kcal mol⁻¹, respectively (Martinez, 2025). Although **Compound 1** displays significantly higher BDE of 29.7 kcal mol⁻¹, it remains under consideration for further DFT screening due to its structural simplicity and absence of bridging groups; substituents will be added to the aryl rings to observe electronic effects of substituents.

Previous mechanistic studies on the photochemically induced radical dehydrocoupling of diorgano(bismuth)chalcogenides, [Bi(di-aryl)EPh], with TEMPO have underscored the pivotal influence of the chalcogen substituent (E = S, Se, Te) on the reaction pathway and efficiency. The photosensitivity of such complexes increases with the atomic numbers of E, reflecting enhanced spin-orbit coupling in heavier chalcogens, whereas the selectivity improves with lighter analogues due to reduced nonradiative decay and tighter control over radical formation (Ramler, 2020). Consequently, SPh is identified as an optimal ligand, offering favorable balance between photoreactivity and selectivity for homolytic cleavage.

To minimize computational cost associated with geometry optimization of bulky molecular bismuth complexes, the effects of different bridging and substituent groups will first be evaluated based on simplified molecular structures which adequately reproduce the key electronic and steric characteristics of the full systems. Such model structures are derived directly from Bi(di-aryl)EPh scaffold, selected for its demonstrated reactivity in radical dehydrocoupling processes. For the fundamental framework shown in **Figure 2**, bridging substituents enumerated in **Figure 1** will be systematically incorporated to examine the influence on the electronic distribution and steric environment of the complexes; the bridging group is denoted by Y in **Figure 2**. Additionally, ortho- and para-directing groups denoted by X in **Figure 2** will be introduced on the aryl rings to probe substituent-dependent effects; for sulfonyl bridging group (Y = SO₂), meta-directing groups will be incorporated on the aryl rings.

In summary, four fundamental ligand frameworks are considered: the unbridged, sulfur-bridged, sulfonyl-bridged, and methyl-bridged systems. For the unbridged framework, both ortho- and para-directing substituents will be introduced at all available positions on the aryl rings to systematically evaluate electronic effects. In contrast, for the sulfur- and methyl-bridged analogues, substituents will be restricted to the para positions to minimize steric interference while preserving conjugative effects. For the sulfonyl-bridged complexes, a single meta-directing

substituent will be introduced at the least sterically hindered position to probe inductive effects without perturbing the overall geometry.

Subsequent analyses will be performed on molecular geometries from X-ray crystallographic data of more complex systems bearing bulky substituent groups. As these detailed models are computationally demanding, the candidate structures selected for such higher-level DFT calculations will be preliminarily narrowed down through the initial screening process of simplified molecular structures.

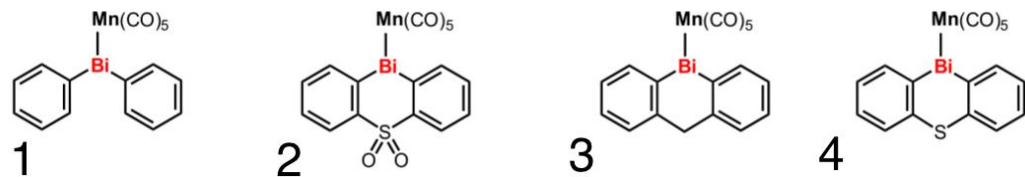


Figure 1: Molecular bismuth complexes with favorable homolytic bond dissociation energies obtained from DFT studies. *Adapted from* “Bismuth Radical Catalysis: Thermally Induced Intramolecular C(sp³)–C(sp) Cyclization of Unactivated Alkyl Iodides and Alkynes,” by S. Martínez, J. Doe, & A. Smith, *ACS Catalysis*, 2025, 15(7), 5123–5134. © 2025 American Chemical Society.

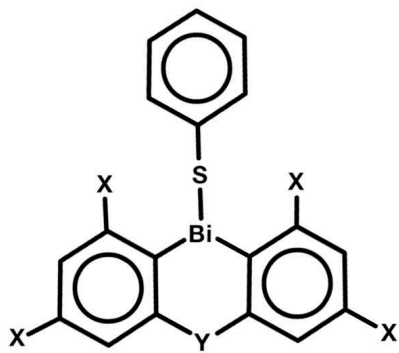


Figure 2: Potential candidates of bismuth molecular complexes [Bi(di-aryl)SPh] for DFT screening (X = NH₂, CF₃, CH₃, H, CH(CH₃)₂, OCH₃) (Y = CH₂, S, SO₂)

II.2 Structural Analysis

All computations will be performed with the ORCA 6.0 program package. To determine the ground-state geometries of the Bi(III) complexes and to closely approximate experimental conditions, geometry optimizations will be performed in benzene solvent with def2-TZVP and def2-SVPD basis sets; def2-TZVP basis set will be primarily used due to its ability to yield the most accurate ground-state geometries, but other cheaper basis sets such as def2-SVPD and def2-SVP may be employed before performing final optimization with def2-TZVP to minimize the computational cost. Relativistic effects for bismuth will be treated with the corresponding effective core potential (ECP). The exchange–correlation functionals such as M06-L, PBE0, and B3LYP will be employed with symmetry constraints utilizing tight self-consistent field (SCF) convergence criteria and tight numerical integration grid settings to ensure accurate evaluation. The M06-L functional, combined with the def2-TZVP basis set and solvent -models, has been reported to yield the most accurate ground-state geometries when compared to experimental X-ray crystallographic data (Martins, 2024). Therefore, the M06-L/def2-TZVP/ECP/CPCM level of theory will be primarily used for all geometry optimizations.

Upon convergence, analytic vibrational frequency analyses will be performed to confirm that the optimized geometries correspond to true ground-state minima on the potential energy surface. Any stationary points are classified as true local minima only if all computed harmonic vibrational frequencies are real; the presence of one or more imaginary frequencies indicate the presence of at least one negative eigenvalue of the mass-weighted Hessian matrix, implying convergence to a first-order saddle point rather than a local minimum.

In cases where spurious imaginary modes are observed despite the use of tight integration grids, or when frequency calculations fail to converge, auxiliary basis set parameters will be adjusted to mitigate linear dependency and numerical instability. Notably, single-point energies exhibited non-negligible deviations ($|\Delta E| = 1.93 \text{ kJ/mol}$) depending on the auxiliary basis set employed as illustrated in **Figure 3**. To maintain consistency across all DFT calculations, the identical auxiliary basis set will be therefore applied for both geometry optimizations and subsequently frequency analyses. By default, AutoAux protocol of ORCA will be primarily utilized to generate appropriate auxiliary basis sets; however, predefined basis sets such def2/J sets may be employed where explicitly defined Coulomb fitting bases improve SCF stability and reduce residual integration errors.

Following confirmation of true local minima , the homolytic bond dissociation energies (BDEs) of the Bi-SPh bonds will be determined from single-point energy evaluations on the optimized single doublet states. The BDE values will be obtained according to:

$$\text{BDE} = E_{\text{Bi}(\text{di-aryl})\cdot} + E_{\text{SPh}\cdot} - E_{\text{Bi}(\text{di-aryl})\text{SPh}}$$

where BDE is determined by the total electronic energy of the optimized closed-shell singlet Bi(III) complex, and the total energies of the resulting Bi-centered and phenylthiyl radicals.

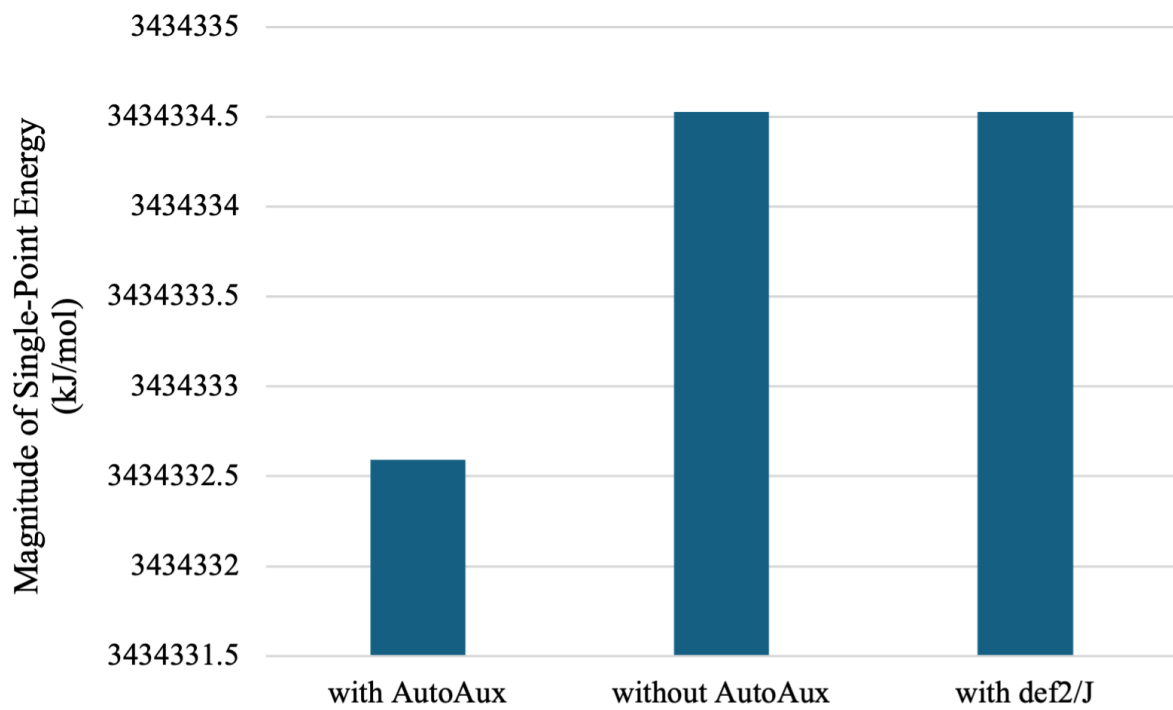


Figure 3: Comparison of single-point energy magnitudes (kJ/mol) of bismuth molecular complexes $[\text{Bi}(\text{di-aryl})\text{SPh}]$ ($\text{X} = \text{H}$, without Y) for different auxiliary basis set configurations

II.3 Quasi-Atomic Bonding Orbital Analysis

Quasi-Atomic Bonding Orbitals (QUAO) are localized orbitals obtained by projecting delocalized molecular orbitals (MOs) onto sets of atomic-centered orbitals, providing a bridge between fully delocalized MOs and atomic orbital interpretations of bonding. QUAO provides insight into electron density distribution and bond character, bridging the gap between fully delocalized molecular orbitals and atomic-centered interpretations; specifically, it provides quantitative analysis of kinetic bond order, electron occupation numbers, and hybridization character, reflecting the contributions of individual atomic orbitals to bonding and antibonding interactions (Ruedenberg et al., 2020). QUAO analysis enables the assessment of bond strengths, radical character, and electronic delocalization in complex molecular systems, making it particularly useful for studying reactive Bi-centered radicals.

II.3.1 Mathematical Background

Let $\{\phi_i\}$ be the set of canonical molecular orbitals and $\{\chi_\mu\}$ be the set of atomic orbitals forming the basis set. Then, QUAOs $\{\phi_A\}$ are constructed via projection operator P_A associated with atom A.

$$\phi_A = P_A \phi_i = \sum_{\mu \in A} |\chi_\mu\rangle \langle \chi_\mu| \phi_i \rangle \quad (1)$$

The occupation number n_i of a QUAO can be obtained from the one-particle density matrix \mathbf{D} expressed in the atomic orbital basis:

$$n_i = \langle \phi_A | \mathbf{D} | \phi_A \rangle \quad (2)$$

Ruedenberg further defined the kinetic bond order K_{AB} between atoms A and B in terms of QUAO overlaps and kinetic energy contributions:

$$K_{AB} = \sum_i \langle \phi_A^{(i)} | \hat{T} | \phi_B^{(i)} \rangle n_i \quad (3)$$

where \hat{T} is the kinetic energy operator and the sum runs over all occupied QUAOs. This formalism allows decomposition of bonding into atomic contributions, providing quantitative insight into hybridization, bond covalency, and delocalization effects.

II.3.2 Computational Procedure

QUAO analyses will be performed in the GAMEES software suite. The ground-state geometries of the molecular bismuth complexes obtained at the M06-L/def2-TZVP/ECP/CPCM level from ORCA 6.0, as listed in the previous section, will be employed for the QUAO analysis. The computational processes are listed below.

For each optimized geometry, the single-point energy calculations will first be executed to obtain the canonical molecular orbitals (MOs) and corresponding density matrices. Subsequently, the molecular orbitals will be transformed into oriented molecular orbitals (OMOs) by diagonalizing the sub-blocks of the density matrix corresponding to each atomic center, aligning each orbital with the principal atomic axes of the bismuth atom and the key atoms of ligands. Such transformation maximizes localization while preserving orthonormality based on kinetic energy minimization (Rudenberg et al., 2020). The resulting OMOs are then projected onto atomic-centered basis functions to derive the QUAOs. Mathematically, the QUAOs are expressed as linear combinations of atomic orbitals where the coefficients are obtained from the least-squares projection of OMOs onto the atomic orbital subspace. The atomic contribution, hybridization coefficients, and kinetic bond orders are then extracted from these coefficients utilizing the post-process modules of GAMESS.

The resulting QUAO data will provide quantitative insight into the distribution of electron density, hybridization character at metal center, and degree of orbital delocalization across the ligand framework, all of which are dependent variables to analyze.

The methodology of QUAO data analysis is demonstrated by the sample results for pyridine as presented in **Figure 4**. In the QUAO framework, each pair of quasi-atomic orbitals represents the localized bonding interactions, classified as σ or π type, depending on the symmetry and nodal structure. The bond order (BO) and kinetic bond order (KBO) values quantify the covalency and kinetic stabilization associated with each orbital pair, respectively. The positive BO values (0.97-0.99) correspond to strong σ -bond such as C-C and C-N linkages, while smaller BO magnitudes correspond to delocalized π -bonds in the aromatic ring system; for instance, the interactions between $C_4N_2\sigma$ and $N_2C_4\sigma$ as shown in **Figure 5** have BO value of 0.979, which indicates presence of strong σ -bond between C-N; such interactions will be denoted as $\{C_4N_2\sigma, N_2C_4\sigma\}$ for the naming convention in the future. The negative BO values reflect antibonding interaction. The negative KBO values reflect the stabilizing kinetic energy contribution of the bonding orbitals, with more negative values indicating stronger kinetic delocalization and greater orbital overlap; for instance, $\{H_{10}C_5\sigma, C_5H_{10}\sigma\}$ has less negative KBO values due to weaker bonding interactions between C and H than those between C and N.

The occupancy (OCC) columns indicate the electron population localized on each atom participating in the bond. For example, $C_4N_2\sigma$ has lower electron density (OCC = 0.87) than $N_2C_4\sigma$ (OCC = 1.13) for $\{C_4N_2\sigma, N_2C_4\sigma\}$, which reflects the polarization of σ -electrons toward the nitrogen atom due to its higher electronegativity.

A similar analysis will be performed on the molecular bismuth complexes to characterize the bonding interactions, hybridization patterns, and orbital delocalization.

Bond Order	KBO (Hf)	QUAO #1	OCC #1 (electron density distribution in first atom)	Orbital I	I - Bonding Type	QUAO #2	OCC #2 (electron density distribution in second atom)	Orbital J	J - Bonding Type	KBO (kJ/mol)	Degeneracy	Total Electron Density
0.9791364	-0.9742447	22	0.8722719	C4N2	SIGMA	13	1.1290388	N2C4	SIGMA	-255.787946	Degenerate	2.0013107
0.9791363	-0.9742442	18	0.872272	C3N2	SIGMA	14	1.1290386	N2C3	SIGMA	-255.7878147	Orbital #1	2.0013106
0.9828763	-0.8512319	30	0.8917976	C6C1	SIGMA	8	1.0063097	C1C6	SIGMA	-223.5224413	Degenerate	1.9981073
0.9828763	-0.8513517	26	0.9917976	C5C1	SIGMA	9	1.0063097	C1C5	SIGMA	-223.5223888	Orbital #2	1.9981073
0.9802941	-0.8500697	25	1.0128025	C5C3	SIGMA	16	1.0055094	C3C5	SIGMA	-223.1857997	Degenerate	2.0183119
0.9802942	-0.8500691	29	1.0128025	C6C4	SIGMA	20	1.0055094	C4C6	SIGMA	-223.1856422	Orbital #3	2.0183119
-0.9744352	-0.6141506	34	0.8531101	H10C5	SIGMA	23	1.1467947	C5H10	SIGMA	-161.24524	Degenerate	1.9999048
0.9744352	-0.6141504	35	0.8531101	H11C6	SIGMA	27	1.1467947	C6H11	SIGMA	-161.2451875	Orbital #4	1.9999048
0.9739772	-0.6126668	31	0.8511401	H7C1	SIGMA	7	1.1513748	C1H7	SIGMA	-160.8556683	Orbital #5	2.0025149
0.9718097	-0.6035317	32	0.8541737	H8C3	SIGMA	15	1.1551481	C3H8	SIGMA	-158.4572478	Degenerate	2.0093218
-0.9718097	-0.6035312	33	0.8541739	H9C4	SIGMA	19	1.1551479	C4H9	SIGMA	-158.4571166	Orbital #6	2.0093218
0.6617704	-0.2615595	21	0.9253321	C4(C6N2)	PI	12	1.1421887	N2(C4C3)	PI	-68.67244673	Degenerate	2.0675208
0.6617689	-0.2615587	17	0.9253323	C3(C5N2)	PI	12	1.1421887	N2(C4C3)	PI	-68.67233669	Orbital #7	2.067521
0.6641117	-0.2350786	24	1.0403107	C5(C1C3)	PI	17	0.9253323	C3(C5N2)	PI	-61.71988643	Degenerate	1.986543
-0.6641159	-0.2350779	28	1.0403109	C6(C1C4)	PI	21	0.9253321	C4(C6N2)	PI	-61.71970265	Orbital #8	1.986543
-0.6661495	-0.2343375	28	1.0403109	C6(C1C4)	PI	10	0.9265252	C1(C6C5)	PI	-61.52531063	Degenerate	1.9668361
0.6661488	-0.2343373	24	1.0403107	C5(C1C3)	PI	10	0.9265252	C1(C6C5)	PI	-61.52525812	Orbital #9	1.9668359

Figure 4: QUAO analysis on kinetic bond order (KBO) and electron density distribution of each pair of quasi-atomic orbitals of pyridine

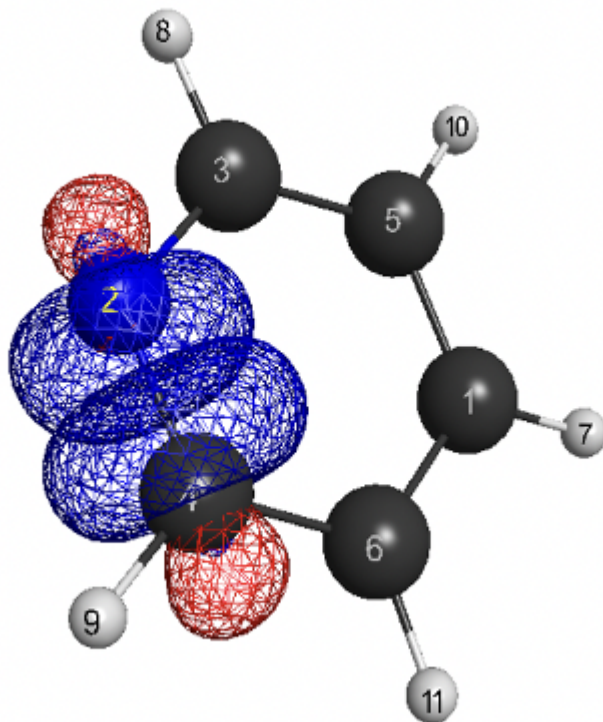


Figure 5: Visualization of the electronic interaction between quasi-atomic orbitals $C_4N_2\sigma$ (22) and $N_2C_4\sigma$ (13)

III. Risk and Safety

The present work involves only computational analyses and poses no immediate safety concerns. All procedures are conducted digitally, without any chemical reagents or laboratory materials. However, the potential future experimental validation may involve the synthesis of Bi(di-aryl)SPh complexes.

A representative pathway involves the reaction of bismuth (III) halide precursor (e.g., BiCl₃) with aryllithium or arylmagnesium halide reagents to form Bi(di-aryl)Cl intermediates, followed by substitution with thiophenol (PhSH) or sodium thiophenoxyde salt (NaSPh). These reagents, particularly aryllithium and Grignard reagents, are highly reactive, moisture-sensitive, and potentially cause thermal burns or fires upon contact with air. Thiophenol also poses acute toxicity and strong odor hazards, requiring careful containment and ventilation.

If experimental synthesis is pursued, all manipulations will be conducted under inert atmosphere (N₂ or Ar) using Schlenk or glovebox techniques in certified chemical fume hood. Appropriate personal protective equipment (PPE), including laboratory coats, gloves, and eye protections, will be worn at all times. All experimental work will be supervised by qualified personnel at the University of Hawaii, adhering to institutional safety protocol. Chemical waste, including halogenated solvents, organolithium residues, and thiophenol-containing materials, will be collected in properly labeled containers and disposed of through the UH Environmental Health and Safety Office (EHSO) in accordance with federal and institutional guidelines.

IV. Conclusion

IV.1 Implications for Computational Studies

The primary datasets for analysis will be derived from the Quasi-Atomic Bonding Orbital (QUAO) results of the optimized geometries. A secondary objective of the research is to compare homolytic bond dissociation energy (BDEs), the definitive energetic index of bond strength, with corresponding QUAO profiles to evaluate potential correlation between the two methods. If a clear statistical correlation is established, the computationally inexpensive QUAO analysis could serve as a practical substitute for the more computationally intensive BDE calculations in future studies. Such correlations would not only streamline computational workflows but also provide more orbital-level understanding of bond stability and radical formation. Moreover, such approaches could be extended toward predictive modeling of other organobismuth complexes and related p-block systems, accelerating the identification of Nobel, stable bonding motifs.

IV.2 Implications for General Studies of Molecular Bismuth Complexes

The outcomes of the study hold broader implications for understanding bonding and reactivity in molecular bismuth complexes. By identifying how orbital localization, hybridization, and spin distribution correspond to measurable bond strengths, the research contributes to a transferable framework for interpreting Bi-X bond activation across diverse ligand environments.

Such insights could refine the general understanding of radical formation and stabilization in organobismuth systems, particularly those relying on single-electron transfer (SET) or homolytic cleavage pathways central to bismuth redox catalysis. QUAO-based descriptors may reveal how electronic delocalization within π -conjugated or electron-donating ligands governs spin distribution and suppresses unwanted radical recombination or dimerization. The orbital-level perspective could therefore guide the rational design of redox-active and sterically tuned ligands, offering predictive control over big-centered radical lifetimes and reactivity.

Beyond the mechanistic significance, these findings align with the broader goals of green and sustainable chemistry. By enabling the rational design of non-toxic, earth-abundant main-group catalysts, the research supports transition away from precious and hazardous transition metals toward environmental benign alternatives.

Citation

Moon, H. W., & Cornella, J. (2022). Bismuth redox catalysis: An emerging main-group platform for organic synthesis. *ACS Catalysis*, 12(2), 1382-1393. <https://doi.org/10.1021/acscatal.1c04897>

Gonçalves, Â., et al. (2024). Bioactive bismuth compounds: Is their toxicity a barrier to their therapeutic and catalytic applications? *International Journal of Molecular Sciences*, 25(3), 1600. <https://doi.org/10.3390/ijms25031600>

Ramler, J., Schwarzmann, J., Stoy, A., & Lichtenberg, C. (2022). Two faces of the Bi-O bond: Photochemically and thermally induced dehydrocoupling for Si-O bond formation. *European Journal of Inorganic Chemistry*, 2022(7), e202100934. <https://doi.org/10.1002/ejic.202100934>

Lichtenberg, C. (2020). Main-Group Metal Complexes in Selective Bond Formations Through Radical Pathways. *Chemistry – A European Journal*, 26(44), 9674–9687. <https://doi.org/10.1002/chem.202000194>

Martínez, S., & Junghanns, M. A., et al. (2025). Bismuth radical catalysis: Thermally induced intramolecular C(sp³)–C(sp) cyclization of unactivated alkyl iodides and alkynes. *ACS Catalysis*. <https://doi.org/10.1021/acscatal.5c0281>

Jomova, K., Alomar, S. Y., Nepovimova, E., Kuca, K., & Valko, M. (2025). Heavy metals: Toxicity and human health effects. *Archives of Toxicology*, 99(1), 153–209. <https://doi.org/10.1007/s00204-024-03903-2>

Suzuki, H.; Ogawa, T. Organobismuth(III) Compounds. In *Organobismuth Chemistry*; Elsevier: Amsterdam, The Netherlands, 2001; pp. 21–245.

Guidez, E. B., Gordon, M. S., & Ruedenberg, K. (2020). Why is Si₂H₂ not linear? An intrinsic quasi-atomic bonding analysis. *Journal of the American Chemical Society*, 142(32), 13729–13742. <https://doi.org/10.1021/jacs.0c03082>